Algorithmic Insufficiency of RSSI Based UKF for RFID Localization Deployment On-Board the ISS

Joshua T. Carnes[1]
Georgia Institute of Technology, Atlanta, GA, 30332

Advisor
Glenn Lightsey[2]
Georgia Institute of Technology, Atlanta, GA, 30332

This work evaluates the application of Unscented Kalman Filter (UKF) to generate stochastic localizations of radio frequency identification (RFID) chips in a sensor poor, highly reflective environment. Localization is done through the application of kNN algorithms and UKF methods to assign to reference RFID tags. The research is conducted in response to the needs of NASA for an application on the International Space Station. While the UKF has been shown to be effective on RFID streams, the sensor poor environment and difficult conditions aboard the ISS cause a loss of localization. This work shows that a UKF alone is insufficient for deployment on the ISS and proposes an alternative. Validation methods are proposed, and initial results are generated. Current industry methods are explored as benchmarks for algorithm performance.

I. Nomenclature

χ	=	Sigma Point
μ_t	=	Estimate Mean at time *t*
Q	=	Covariance Matrix of Process Noise
P_t	=	Covariance Matrix of Estimate at time *t*
R	=	Covariance of Additive Measurement Noise
K_t	=	Kalman Gain
n	=	Dimension of State Space
α, κ, β	=	Scaling Parameters
w_m, w_c	=	Weigh Variables
g	=	Control Function
h	=	Measurement Function
$\hat{z}_t$	=	Predicted Observation at time *t*
$\overline{P_t^{x,z}}$	=	State and Observation Cross Covariance
$\boldsymbol{\Theta}$	=	Received Signal Strength Indicator (RSSI) Values from Reference Tags to Antennae
e_j	=	Euclidean Distance between Reference Tags and Tracking Tags
$RMSE$	=	Root Mean Square Error

II. Introduction and Motivation

The International Space Station ("ISS") is a critical international test bed for new technologies and areas of research. In support of the ISS's research missions, large quantities of tools and specific items ("Items") must be brought aboard. Once these Items are aboard, the crews must categorize, label, and stow all these Items to ensure current and replacement crews can easily find and access them. Due to the difficulty of working and maneuvering in a micro-gravity environment, frequent crew turnover, and each crew developing their own methodology for stowing Items, such Items can be easily misplaced, mislabeled, or errantly stowed causing a reduction in crew productivity.

[1] Master's Student, Department of Aerospace Engineering, Georgia Institute of Technology, Student Member AIAA
[2] Professor, Georgia Institute of Technology, AIAA Fellow

To remedy this problem, NASA has begun to introduce Radio Frequency Identification ("RFID") tags and sensors onto the Items brought aboard the ISS. The tags have been introduced to enable swift and accurate location of the Items.

Because of the harsh environment, many RFID tags are not detected by the RFID reading scanners. Physical methods, such as additional RFID readers, could be used to solve the problem, however limitations on installation time and mass aboard the ISS, render additional physical installations unlikely. To enhance the probability of success regarding the use of RFID systems aboard the ISS and other space vehicles, further research and development is needed to increase the success rate of such systems. One possible technique is the use of localization.

Localization refers to the estimation of a state or states, typically position, from recorded, often noisy, observations. Various algorithms have been developed to perform localization over uncertain measurements. These algorithms are composed commonly of two components: the motion model, which describes how states evolve over time, and a measurement model that describes how states influence sensor measurements. RFID localization is an ongoing area of research for inventory management systems where large movement of cargo must be tracked.[1] The ISS presents a unique challenge in the area of RFID localization due to the extreme limitation of sensors and the difficult, reflective environment of space vehicles and habitats.

The primary issues facing the current RFID localization systems are multi-path propagation and environment reflectivity. This creates measurement models that are difficult to evaluate, as the uniqueness of measurements in the environment is greatly diminished. Additionally, there are issues of loss of signal with multi-agent detection. Here, a tag can be read by a scanner far from the original item while not by the closest scanner, which further erodes trust in the measurement model.

This research has impact outside of NASA's mission requirements. The inventory management market is a multi-billion-dollar industry that stands to be improved by this line of research.

III. Current State of the Art

A. RFID Technology and Network

RFID technology uses two primary components: the reader which sends out a signal to query the environment and detects responses, and the RFID tags which respond to the signal by replying. There are several varieties of RFID tags, two of which are important for this research. First is the passive tag which is smaller, cheaper, and most importantly has no internal energy supply. This type has elements that either backscatter the reader's signal or use it to power their own return signal. Passive tags are therefore very short-range devices. Another tag type is a semi-passive tag. These tags have no onboard sensors like the passive tags but are fitted with their own power source. Semi-passive tags are necessarily larger, more expensive to construct, and have a limited deploy time. The tradeoff for this is the ability to emit a far stronger signal to the reader. These two tags are of importance to this research as they are the types of tags currently deployed aboard the ISS. The small passive tags are deployed on most item's being brought aboard, while the semi-passive tags are attached to Cargo Transfer Bags (CTBs). CTB's serve dual purposes as transport and storage containers for much of the cargo. Lastly an additional component, a server, can be added to the RFID system to make it into a network. The server collates the detected tag information from all readers. It is on this stream of information that localization is performed.

Several pieces of additional information can be transmitted back to readers besides tag identities, including: Received Signal Strength Indicator (RSSI), Received Signal Phase Indicator (RSPI), Time of Arrival (TOA), and Time Difference of Arrival (TDOA). For this research, RSSI is utilized as this is the measurement available from the current ISS installation.

RSSI based localization operates by using the attenuation of RF signal strength over distance to estimate the distance between a reader and tag. Position is then estimated via triangulation from at least three readings. Alternatively, instead of attempting to calculate distance directly, environment mapping methods can be used. Environment mapping consists of using two phases, a 'finger-printing' step that is conducted before the data RFID gathering step. With environment mapping, the location is estimated by utilizing the figure-print of the environment. The two most prominent algorithms for environment mapping are k-nearest-neighbor (kNN) and various stochastic approaches.

In kNN, the location of a dynamic tag is calculated by minimizing the RMSE in signal space between the dynamic tag and the k nearest tags with known location. The location of the tag is then estimated as the weighted centroid of these fixed tags, also known as reference tags (RT).

Stochastic methods consist of compartmentalizing the environment into discrete regions, utilizing Bayes formula and a posteriori estimates to evaluate the most probable region. These methods typically require some form of supervised learning to be effective.

B. RFID Localization

Several algorithms exist for RFID localization. One of the most used for environment mapping applications is Landmarc, which uses kNN with fixed position RT to track the dynamic tag using:

$$e_j = \sqrt{\Sigma_{i=1}^{n}\left(\theta_{j,i} - S_i\right)^2} \tag{1}$$

Where n is defined as the number of readers, S_i the RSSI of the dynamic tag as seen by reader i, and $\theta_{j,i}$ is the RSSI of the RT j as seen by reader i. [2] Several additional methods are summarized in Table 1.

Table 1. RFID Localization Summery [2]

Localization Scheme	Positioning Algorithm	Reference Tags	Target	Space Dimension
SpotON (2000)	RSSI Lateration	No	Active	3-D
SAW ID-tags (2003)	TOA lateration	No	Passive	2-D
LPM (2004)	TDOA weighted mean squares	No	Active	2-D
RSP (2007)	RSP/AOA	No	Passive	2-D
Landmarc (2003)	kNN	Yes	Active	2-D
VIRE (2007)	kNN	Yes	Active	2-D
Simplex (2007)	kNN optimizaiton	Yes	Active	3-D
Kalman Filtering (2007)	RSSI mean squares and kalman filtering	Yes	Active	2-D
Scout (2006)	RSS Bayesian approach	Yes	Active	2-D
3-D Constraints (2008)	Rage-free optimizaiton	No	Active	3-D

Of importance for this research is Kalman Filtering. The standard Kalman filter is a two-step algorithm, a propagation (prediction) step and an evaluation (error update) step. To perform Kalman Filtering, assumptions are made that the noise of measurements is a gaussian random process and a Markov assumption is made to decouple time dependence. The standard Kalman filter is based on a linear propagation dynamic model and a linearized Extended Kalman Filter (EKF) may be used to accommodate second order non-linearities. In the RFID localization problem, however, the non-linearities are higher than second order. To address this issue, the Unscented Kalman Filter (UKF) has been developed. Instead of using linearized models in the states, linearization is conducted through 'through stochastic linearization'. [3] Here, Sigma Points are used, which are placed at the estimated states mean and two at each one-sigma value on the axis of covariance in n dimensions, for a total of $2n + 1$ Sigma Points. These Sigma Points are passed through the filter as described in Eq. 2 – Eq. 13. First, the Sigma Points are placed along the previous steps mean and along both directions of each of the n dimensions, as shown in Eq. 2. These points are passed through the control function g to generate an a posteriori distribution in Eq. 3.

$$\chi_{t-1} = \begin{bmatrix} \mu_{t-1} & \mu_{t-1} + \gamma\sqrt{P_{t-1}} & \mu_{t-1} - \gamma\sqrt{P_{t-1}} \end{bmatrix} \tag{2}$$

$$\bar{\chi}_t^* = g(u_t, \chi_{t-1}) \tag{3}$$

Where $\sqrt{P_{t-1}}$ is the row or column vector of the matrix square root of P_{k-1}. The propagated mean and covariance for the Sigma Points is then calculated in Eq. 4 – 5, with weights defined in by:

$$\gamma = \sqrt{n + \delta}$$

$$\delta = \alpha^2(n + \kappa) - n$$

$$w_m^{[0]} = \frac{\delta}{n + \delta}$$

$$w_c^{[0]} = \frac{\delta}{n+\delta} + (1 - \alpha^2 + \beta)$$

$$w_m^{[i]} = w_c^{[i]} = \frac{1}{2(n+\delta)} \; for \; i = 1, \ldots, 2n$$

$$\bar{\mu}_t = \sum_{i=0}^{2n} w_m^{[i]} \bar{\chi}_t^{*[i]} \tag{4}$$

$$\bar{P}_t = \sum_{i=0}^{2n} w_c^{[i]} \left(\bar{\chi}_t^{*[i]} - \bar{\mu}_t\right)\left(\bar{\chi}_t^{*[i]} - \bar{\mu}_t\right)^T + Q \tag{5}$$

Where n represents the dimensionality of the estimation, α and κ are scaling parameters for the distance along the covariance axes the sigma points spread, $w_m^{[0]}$ controls the relative weight of the mean term to the estimated mean $\bar{\mu}_t$, and $w_c^{[0]}$ similarly controls the relative weight of the mean terms on the estimated covariance $\bar{P}_t$.

New Sigma Points are then placed at the placed at the newly propagated mean and covariance in Eq. 6. These new Sigma Points can be used to estimate the uncertainty of the propagated system.

$$\bar{\chi}_t = \left[\bar{\mu}_t \quad \bar{\mu}_t + \gamma\sqrt{\bar{P}_t} \quad \bar{\mu}_t - \gamma\sqrt{\bar{P}_t}\right] \tag{6}$$

The Sigma Points are then passed through the measurement model (h) in Eq. 7. The predicted observation is then calculated in Eq. 8 with predicted uncertainty calculated in Eq. 9, where R is the covariance of the additive measurement noise.

$$\bar{Z}_t = h(\bar{\chi}_t) \tag{7}$$

$$\hat{z}_t = \sum_{(i=0)}^{2n} w_m^{([i])} \bar{Z}_t^{[i]} \tag{8}$$

$$S_t = \sum_{i=0}^{2n} w_c^{[i]} \left(\bar{Z}_t^{[i]} - \hat{z}_t\right)\left(\bar{Z}_t^{[i]} - \hat{z}_t\right)^T + R \tag{9}$$

Last, to calculate the Kalman gain, the cross-covariance between state and observation are calculated in Eq. 10 and used to finally calculate the Kalman gain in Eq. 11. The mean and covariance of the new time step is then calculated in Eq. 12 – 13. A further treatment of UKF is can be found at [3].

$$\bar{P}_t^{x,z} = \sum_{i=0}^{2n} w_c^{[i]} \left(\bar{\chi}_t^{[i]} - \bar{\mu}_t\right)\left(\bar{Z}_t^{[i]} - \hat{z}_t\right)^T \tag{10}$$

$$K_t = \bar{P}_t^{x,y} S_t^{-1} \tag{11}$$

$$\mu_t = \bar{\mu}_t + K_t(z_t - \hat{z}_t) \tag{12}$$

$$P_t = \bar{P}_t - K_t S_t K_t^T \tag{13}$$

The UKF framework can then be adapted for the position estimation using RSSI measurements of RT and active tags (AT). As shown in [3], let t represent a vector of the RSSI measurements of one unknown tag by M readers in the form of Eq. 14:

$$t = [t_1\ t_2\ \ldots.\ t_M] \tag{14}$$

Additionally, let the matrix of RSSI measurements from the N reference tags by the M readers be written as Eq. 15

$$\boldsymbol{\Theta} = \left[\begin{pmatrix} \Theta_{11} & \cdots & \Theta_{1M} \\ \vdots & \ddots & \vdots \\ \Theta_{N1} & \cdots & \Theta_{NM} \end{pmatrix}\right] \tag{15}$$

Then, the Euclidian distance in RSSI space between the observed tags and reference tags can be calculated by:

$$e_j = \sqrt{\sum_{i=1}^{M} \left(\Theta_{ji} - t_i\right)^2} \tag{16}$$

The kNN approach to localization would then be to apply Eq. 17 – 18 for estimation.

$$w_i = \frac{\frac{1}{e_i^2}}{\sum_{i=1}^{k}\left(\frac{1}{e_i^2}\right)} \tag{17}$$

$$(x, y) = \sum_{i=1}^{k} w_i\left(x_{RT_i}, y_{RT_i}\right) \tag{18}$$

Instead, as was done in [3], the measurement function h will use the kNN output as an input to the UKF. Therefore, the input to the measurement function consists of the distances, d_i, calculated from the RSSI measurements and the position of the k nearest neighbors as calculated previously.

IV. Experiment Overview

This experiment is conducted to demonstrate that current methods of localization will prove insufficient for deployment aboard the ISS. This will motivate the development of the algorithm discussed in Future Work.

For this work, a testing area was created. A $12x12$ ft area was prepared as shown in Figure 1, with a grid of reference points placed every yard. Passive backscatter RFID tags were used with the Alien 9900 RFID reader operating in UHF. Two plate Alien antennas were used to better receive area signals. Important Alien 9900 settings are summarized in Table 3. The reference tag and antenna configuration can be seen in 2D plane in Figure 2. Position of readers are summarized in Table 2.

Figure 1. Experiment Area

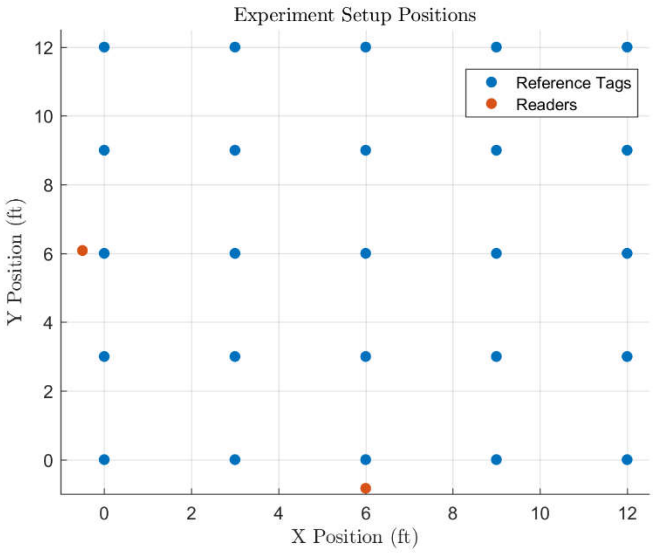

Figure 2. Experiment Setup Positions

Table 2. Alien Reader Settings

Reader Setting	Value
Frequency	928 MHz
Transmitter Output Power	1 Watt

Table 3. Antenna Location Summery

Antenna	X (in)	Y (in)	Z (in)
0	72	-10.00	81
1	-6	73	70

The RFID readers were placed out of plane for better RFID signal recovery. The tracked object was constrained to a plane 41 in off the ground for similar reasons.

Original plans for using a set of fixed RFID reference tags was abandoned for two reasons. First, the high variability between different tags measured by the Alien readers caused tags in similar positions to emit widely varying RSSI measurements. Second, Alien readers struggle with collision issues with multiple antennas. Therefore, only a small subset of tags was observed when placed in the testing environment despite all tags being individually observable. To avoid these issues, the space was fingerprinted with a single tag. RSSI measurements of the tag in the test plane (41 in off the ground) were taken for 10 seconds at each of the reference tag positions. The average of these measurements was taken as calibration measurement for that location. A matrix of calibration measurements for each position and for each antenna was then constructed for use in the UKF. This procedure should yield similar results to having a set of reference tags in the environment. [2] Space finger printing results can be seen in Figure 3.

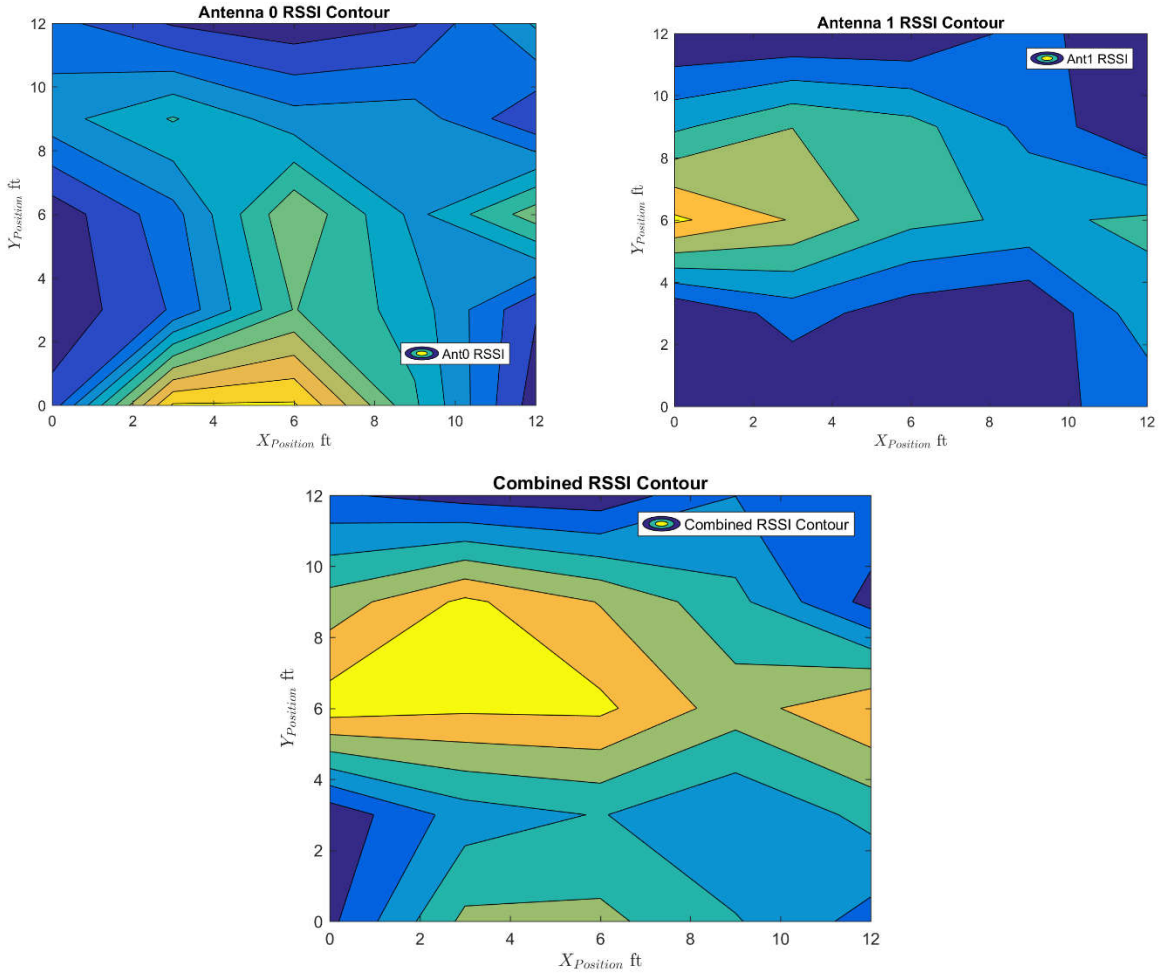

Figure 3. Reference Tag RSSI Contour

Once the space was fingerprinted, the tag was moved at constant velocity along predefined paths using a track. The track trajectory position data is shown in Figure 4, with start and end position data along with velocity magnitude data shown in Table 4. A total of eight runs were conducted with 3 separate configurations.

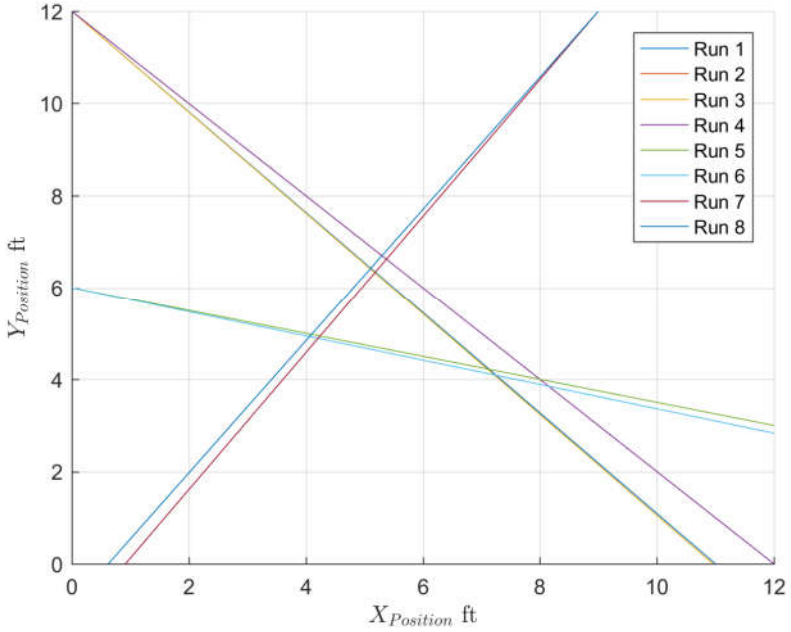

Figure 4. Ground Track Position Data by Run

Table 4. Location and Velocity Summery by Run

Run	X_i ft	Y_i ft	X_f ft	Y_f ft	V_x ft s^{-1}	V_y ft s^{-1}
1	0.00	12.00	11.00	0.00	0.71	-0.78
2	0.00	12.00	12.00	0.00	0.85	-0.85
3	0.00	12.00	10.96	0.00	0.89	-0.97
4	0.00	12.00	12.00	0.00	0.28	-0.28
5	0.00	6.00	12.00	3.00	0.75	-0.19
6	0.00	6.00	12.00	2.83	0.90	-0.24
7	9.00	12.00	0.92	0.00	-0.43	-0.63
8	9.00	12.00	0.63	0.00	-0.49	-0.71

Time, receiving antenna, and RSSI measurements were output to the TCP port of the connected computer and later imported into MATLAB for post processing and analysis. The data was then grouped by receiving antenna, discretized into $0.1s$ intervals.

Once the data had been preprocessed, the measurement and state transition functions to the UKF were input into MATLABs UKF tool. The states are position and velocity, shown in Eq. 19. A linear state transformation was used and is shown in Eq. 20, where dt is the timestep.

$$x = \begin{bmatrix} x_{pos} \\ y_{pos} \end{bmatrix} \tag{19}$$

$$x_t = x_{t-1} + dt * V \tag{20}$$

As per [4] and [5], the hyperparameters for the UKF were set as shown in Eq. 21:

$$\Omega = [\alpha, \beta, \kappa] = [0.001, 2, 0] \tag{21}$$

Position over time was propagated from v and a small time interval, $dt = 0.1\ s$. Lastly, the measurement model was specified. As per [6], the distance between the M^{th} reader and the i^{th} observation tag can be calculated in Eq. 22:

$$d_{Mi} = \sqrt{(x_M - x_i)^2 + (y_M - y_i)^2 + \left(z_M - \frac{41}{12}\right)^2} \tag{22}$$

Next, RSSI values must be converted to distances for the correction step of the UKF. Transforming RSSI values into distances is notoriously difficult. The calculated distances are the single largest source of error within this project. The calculation is done through Eq. 23.

$$\hat{d}(t) = 10^{\frac{d_0(RSSI(d_0) - RSSI(d_t))}{10q}} \tag{23}$$

Where d_0 is a 'close-in' reference distance, $RSSI(d_0)$ is the RSSI value at the reference distance, and q is the path loss exponent, usually between 1.6 to 6.5 based on configuration [6]. For the analysis performed in this experiment a value of $q = 2.7$ was empirically determined to give the best results. For this experiment, d_0 is taken to be the distance between a reader and the closest reference tag, and $RSSI(d_0)$ is taken as the RSSI value for the tag.

V. Experiment Results

To first validate the system model, the UKF was used as a propagator. Results from a sample run can be seen in Figure 5, where the initial position was assigned to be within inches of the true starting point. Velocity of the system is not being estimated in this work. Instead, the true velocity of the system is fed into the state transition function. The system estimates are extremely close to that of the cart, which validates the initialization and propagation methods.

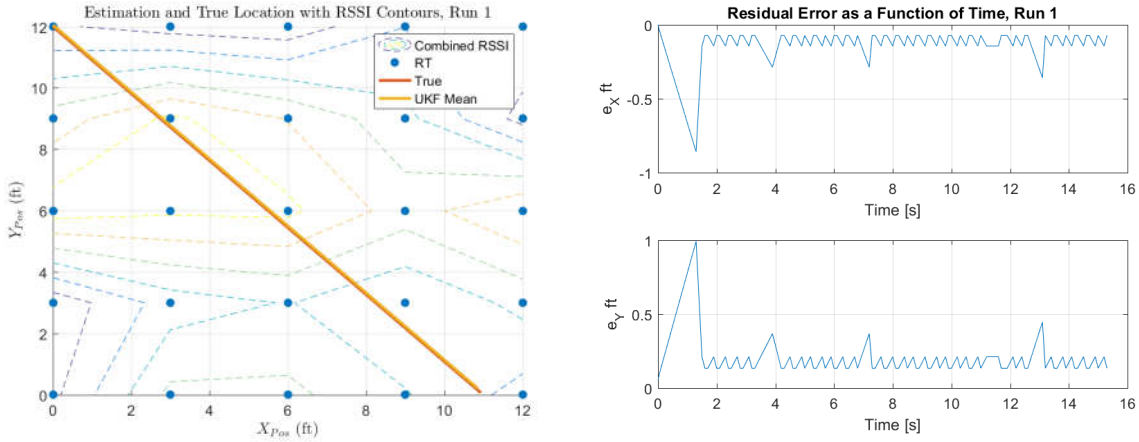

Figure 5. Propagation Performance

A UKF may operate with either additive or non-additive noise. First, additive noise in both the motion and sensor model are considered. For robustness, the additive sensor model noise parameter R is initialized as $N(\mu, \sigma^2) = N(0,5)$. This was chosen as the space was 12 ft by 12 ft, corresponding to a maximum distance of ~15 ft. Similarly, the additive process noise term was given by $Q = N(\mu, \sigma^2) = N(0, \| V \|)$. This produced results like those in Figure 6, where 6a shows the true, measured and estimated distance from each reader over time, 6b shows the mean estimate and true position in the X,Y plane, 6c shows the residual error over time for each component and 6d shows the position components over time. The RMSE per run plotted in Figure 7.

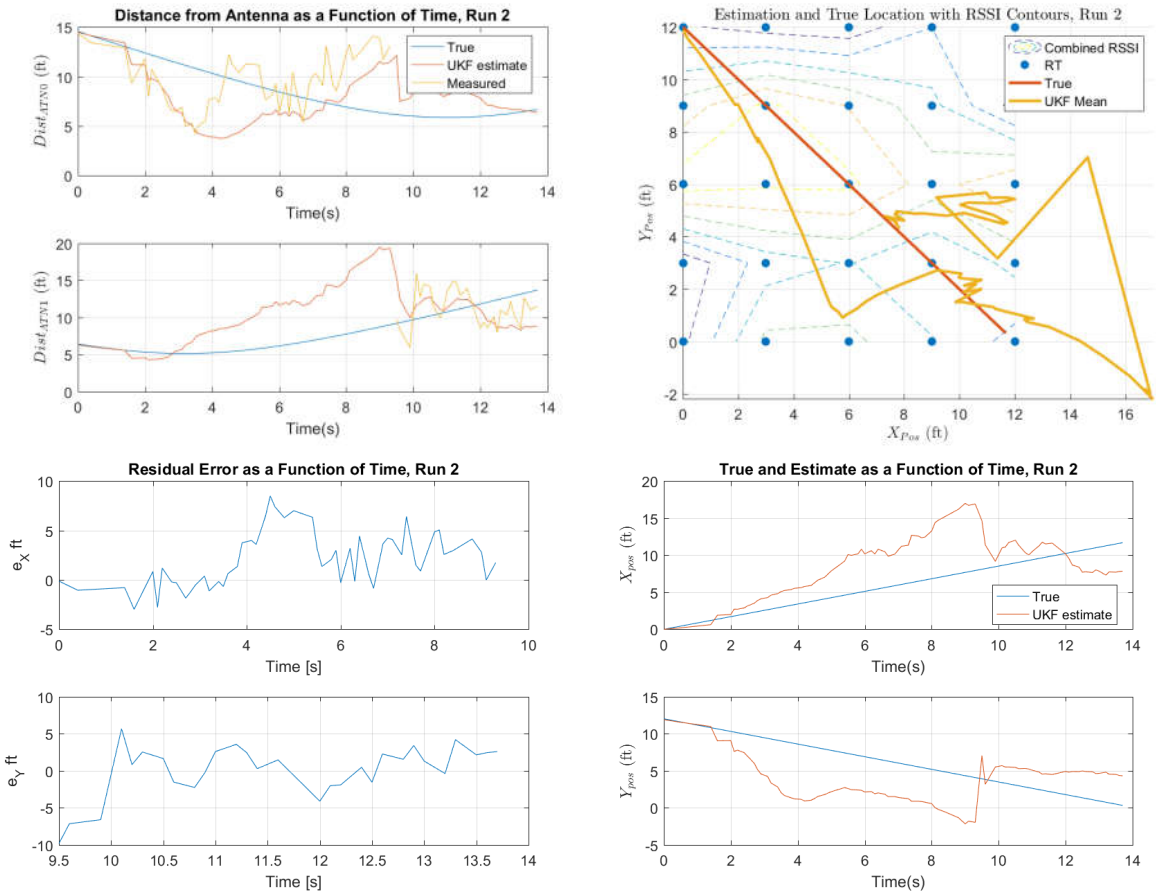

Figure 6. Additive UKF Performance, Run 2

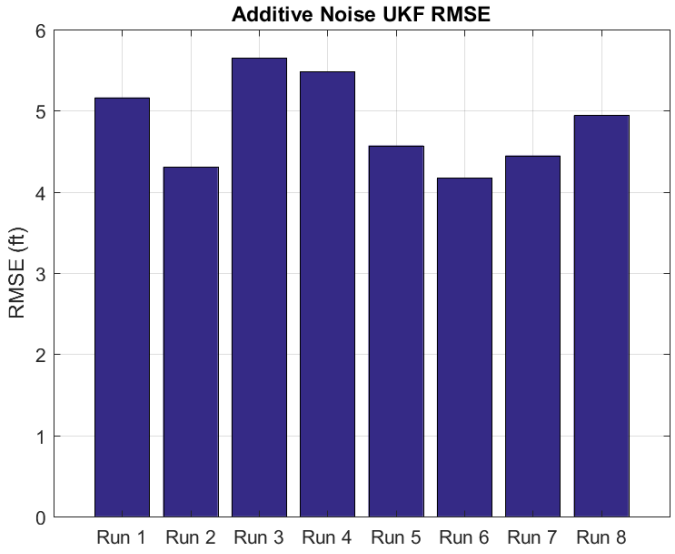

Figure 7. Additive Noise UKF RMSE Per Run

The inferior performance seen is explained by the non-linearity of RSSI localization and the poor correlation between RSSI measured distance and the true distance. Therefore, to improve results, a non-additive noise version of both the sensor and state transition functions are used.

For the non-additive state transition function, the noise parameter was initialized to the same values as those in the additive version. This can be seen in Eq. 24. The state transition noise parameter was then used as the uncertainty of the velocity of the system.

Next, the measurement model was modified. Instead of being additive, the noise parameter was used as multiplicative noise in the distance term. The updated measurement model is shown in Eq. 24. The non-additive noise term was initialized to $N(\mu, \sigma^2) = N(0,0.3)$ to account for the large discrepancies between measured distance and estimated distance.

$$x_{new} = x_{old} + dt * (Velocity + Q) \tag{24}$$

$$d_{iM} = (1 + R)\sqrt{(\hat{x} - x_M)^2 + (\hat{y} - y_M)^2 + \left(\frac{41}{12} - z_M\right)^2} \tag{25}$$

The non-additive UKF was then tested over the sample runs. Results for the same run as the additive noise example can be seen in Figure 8. A marked improvement in performance is notable between the two. This can be seen in the plot of the RMSE per run in Figure 9. The difference in performance has to do with the choice between the multiplicative and additive noise. This is illustrated in Figure 10, which shows the RMSE error per run per covariance configuration. The configurations are summarized in Table 5.

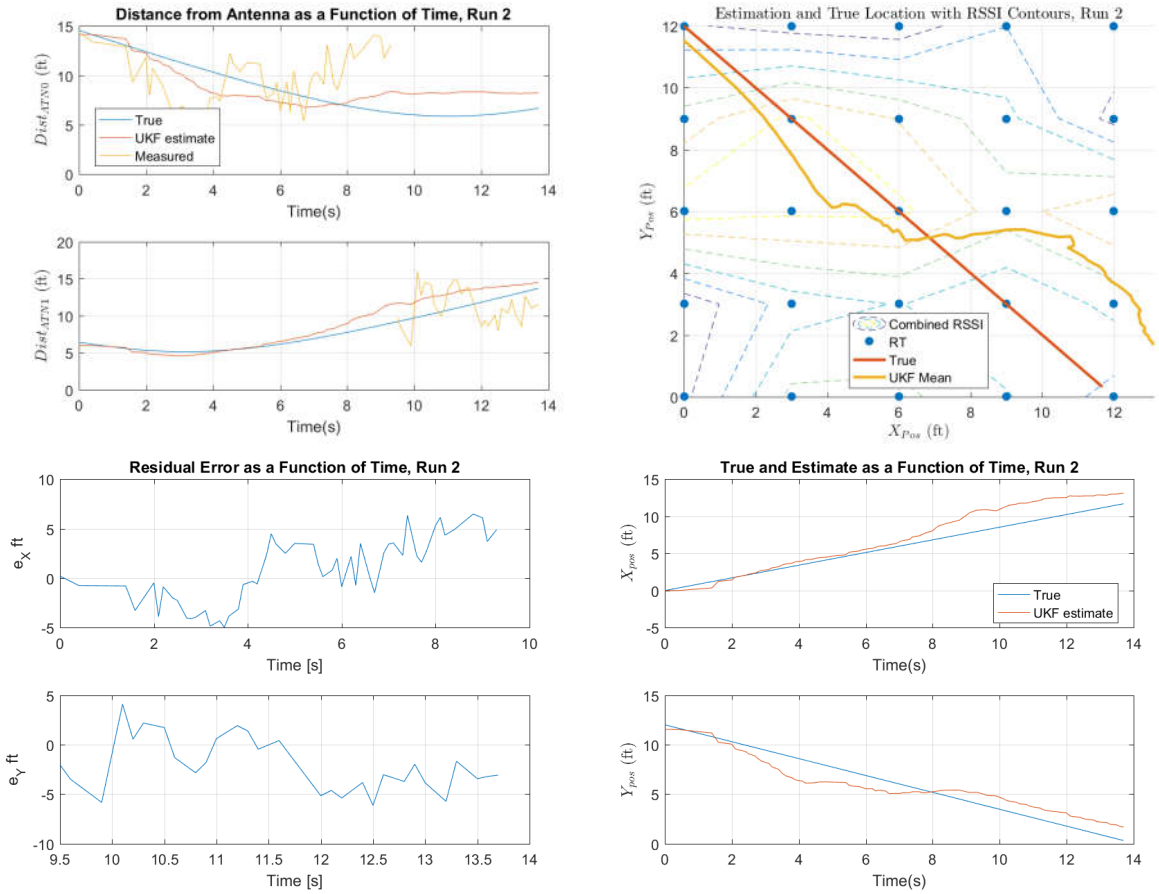

Figure 8. Multiplicative Noise and Transition Model UKF Performance, Run 2

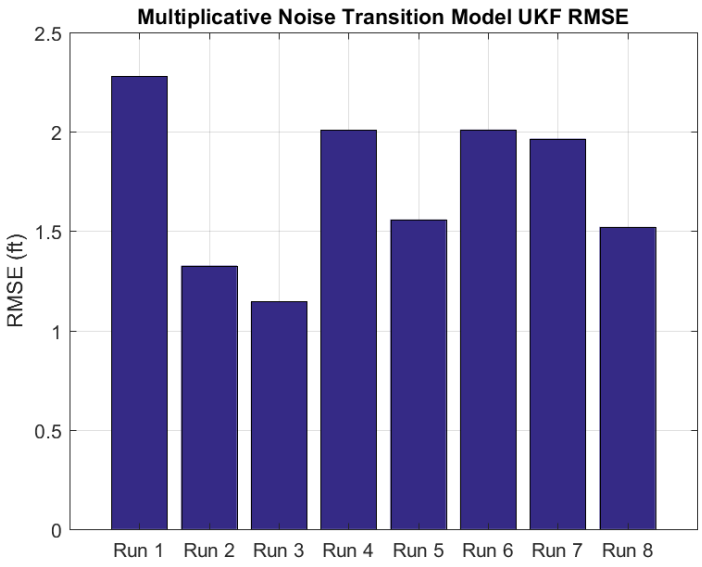

Figure 9. Multiplicative Noise and Transition Model Noise UKF RMSE

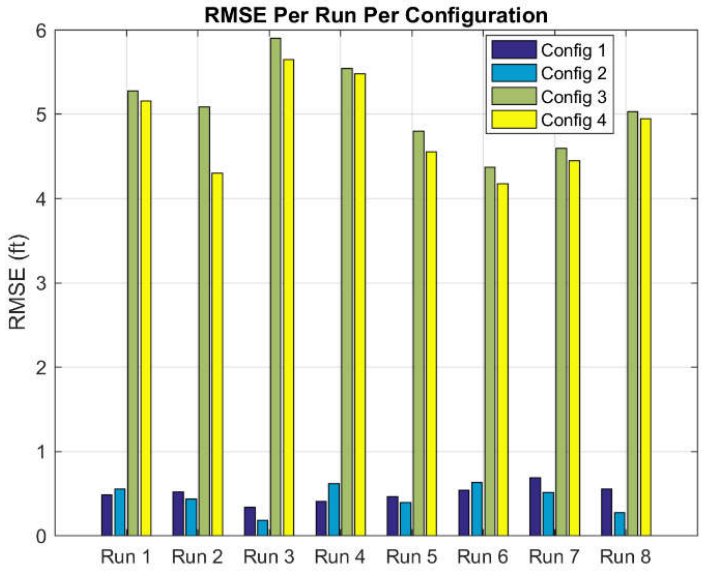

Figure 10. RMSE Per Run Per Configuration

Table 5. Configuration Summery

Configuration	Uncertainty Type	Covariance Parameter
1	Multiplicative	0.5
2	Multiplicative	5
3	Additive	0.5
4	Additive	5

Of note is the RSSI measured distance, calculated by Eq. 23, and the true distance as shown in Figure 8a. The difference between these values shows the primary issue with RSSI only measurements, namely that RSSI values in an indoor environment are strongly influenced by multipath and signal reflection issues that diminish the direct correlation with distance as shown. The weakened correlation causes the UKF estimate to diverge from the real system over short periods of time. There are several variables that cannot be accounted for in a general system, such as angle to receiver that is hard to map without deliberate calibration which is unavailable for the specific application to the ISS.

VI. Conclusion and Future Work

The UKF is an extremely versatile and useful tool and has been shown in simulation to work for certain classes RFID localization problems. The ISS is an environment in which current RSSI based UKF struggles to operate because indoor environments with high reflectivity and multi-path signal propagation are difficult to model with RSSI ranging techniques. Non-linear and hard to quantify terms dominate in these environments, making RSSI based UKF range techniques outside of the lab setting difficult. An adequate sensor model is non-trivial and must be developed for each environment, which is not cost effective for ISS deployment. Therefore, an alternative approach to locating missing supplies aboard the ISS is needed.

For the future, these results should be verified again using alternative RSSI ranging techniques such as gaussian smoothing.[7] These alternative methods might provide a smoother distance estimates that are more strongly correlated with RSSI values. In situ measurements from the intended environment are pending release by NASA and can be used to verify the results above.

References

1. Ku, W. S., Chen, H., Wang, H., and Sun, M. T. "A Bayesian Inference-Based Framework for RFID Data Cleansing," *IEEE Transactions on Knowledge and Data Engineering* Vol. 25, No. 10, 2013, pp. 2177-2191. doi: 10.1109/TKDE.2012.116
2. Bouet, M., and Santos, A. L. d. "RFID tags: Positioning principles and localization techniques," *2008 1st IFIP Wireless Days*. 2008, pp. 1-5.
3. Nick, T., and Götze, J. "Localization of passive UHF RFID Labels with Kalman Filter," *Advances in Radio Science* Vol. 10, 2012, pp. 119-125. doi: 10.5194/ars-10-119-2012
4. Thrun, S., Burgard, W., and Fox, D. *Probabilistic Robotics (Intelligent Robotics and Autonomous Agents)*: The MIT Press, 2005.
5. Sakai, A., and Kuroda, Y. "Discriminative Parameter Training of Unscented Kalman Filter," *IFAC Proceedings Volumes* Vol. 43, No. 18, 2010, pp. 677-682. doi: https://doi.org/10.3182/20100913-3-US-2015.00063
6. Jin, X.-b., Chun-Xue, N., Yan, S., and Ting-Li, S. *Maneuvering Target Tracking with UKF and EKF for Indoor RFID System*, 2016.
7. Xu, H., Ding, Y., Li, P., Wang, R., and Li, Y. "An RFID Indoor Positioning Algorithm Based on Bayesian Probability and K-Nearest Neighbor," *Sensors (Basel, Switzerland)* Vol. 17, No. 8, 2017, p. 1806. doi: 10.3390/s17081806